Fellenius, B.H., 2025. Revisiting Mansur and Kaufman (1956). Pile tests, Sill structure, Old River, Louisiana. Journal of the Deep Foundation Journal, 19(1) 8p.

Case Study

Revisiting Mansur and Kaufman (1956): Pile Tests, Low Sill Structure, Old River, Louisiana

Bengt H. Fellenius[1]*

Abstract: Static pile loading tests were conducted in the 1950s and 1960s as part of efforts to improve infrastructure along the Mississippi River and its tributaries. The resulting test reports led to several influential papers published in ASCE journals and conferences, which became foundational references in the development of pile analysis and design practices. Mansur and Kaufmann (1956) documented one of the earliest test series to incorporate instrumentation for measuring strain along the pile under applied loads, allowing for interpretation of axial force distribution and differentiation between shaft and toe resistances. Their paper continues to offer valuable insights for modern practice. To that end, selected test results have been digitized and reanalyzed to illustrate the early understanding of load transfer mechanisms and to contextualize their work in light of concepts not yet recognized at the time—such as residual force, the importance of accurately separating shaft and toe responses, and the application of effective stress conditions. Notably, pile group behavior was not addressed in these early studies.

Introduction

The response of a piled foundation to applied loads depends on both shaft resistance—governed primarily by soil shear—and toe resistance, which is influenced by compressive strength and displacement behavior. While both components are affected by a range of factors including geology, shear strength, and compressibility, they exhibit distinct force–movement responses. Current understanding has evolved over decades through full-scale static loading tests on instrumented single piles, allowing the separation of shaft and toe contributions. Such instrumentation became feasible only around the 1950s, with the study by Mansur and Kaufman (1956) on static compression and tension tests for the Lock and Dam 4 sill structure in the Mississippi River standing as a pioneering case history paper. At the time, the most commonly employed instrumentation consisted of telltale-recorded pile compressions that then were converted to strain, ε, which, in turn was converted to axial force by multiplication with the pile's axial EA-parameter over a minimum 10-ft section length. However, as reported in the study, the researchers developed instrumentation capable of directly measuring strain at discrete depths. The tests were performed "*to determine the required type size and length of piles necessary to carry the design compression and tension loading without any significant movement of the structure*". the study offered early insight that safe design loads for piled foundations should be based on the settlement acceptable to the supported structure, rather than relying on arbitrary safety factors applied to an often loosely defined "capacity".

As detailed by Mansur et al., 1964 and Mansur and Hunter, 1970, the tests were a part of the study for upgrading the Mississippi River and tributaries and involved constructing 19 locks and dams supported on piled foundations and a very large series of separate projects, justifying detailed pile tests. The piles would be driven in dewatered excavations, but be submerged during the operational life of the structures. Thus, the use of the back-analysis of the loading tests for the final design needed to consider the effective stress distribution during the tests and during the long-term. Feagin (1948) presented some of the information necessary for piled foundation design of the lock and dam foundations, including settlement observations on prior structures over 10 to 15 years of service.

Soil Profile and Test Piles

The tests were conducted off-site. The original soil profile consisted of a 15-meter-thick upper layer of clay and silt, underlain by 12 meters of clay (with a natural water content (w_n) of 30%), followed by 4 meters of silt and sand, and over 15 meters of very dense sand. To replicate soil conditions similar to those at the project site, the area around the test piles—measuring 30 by 45 meters—was excavated to a depth of 15 meters prior to pile installation. As a result, the soil at the test location was no longer normally consolidated, and the tests were performed under prestressed soil conditions. However, Mansur and Kaufman did not clarify whether similar prestressing was present at the actual project site.

The groundwater table was located at the bottom of the excavation, with pore pressure distributions ranging from hydrostatic conditions to an artesian head of 1.5 meters in the

[1] Consultant, Sidney, Canada, V8L 2B9
* Corresponding author, email: bengt@fellenius.net

Print ISSN: 1937-5247 Online ISSN: 1937-5255
Published by Deep Foundations Institute
Received 10 May 2024; received in revised form 6 March 2025; accepted 3 April 2025
https://doi.org/10.37308/DFIJnl.2024510.309

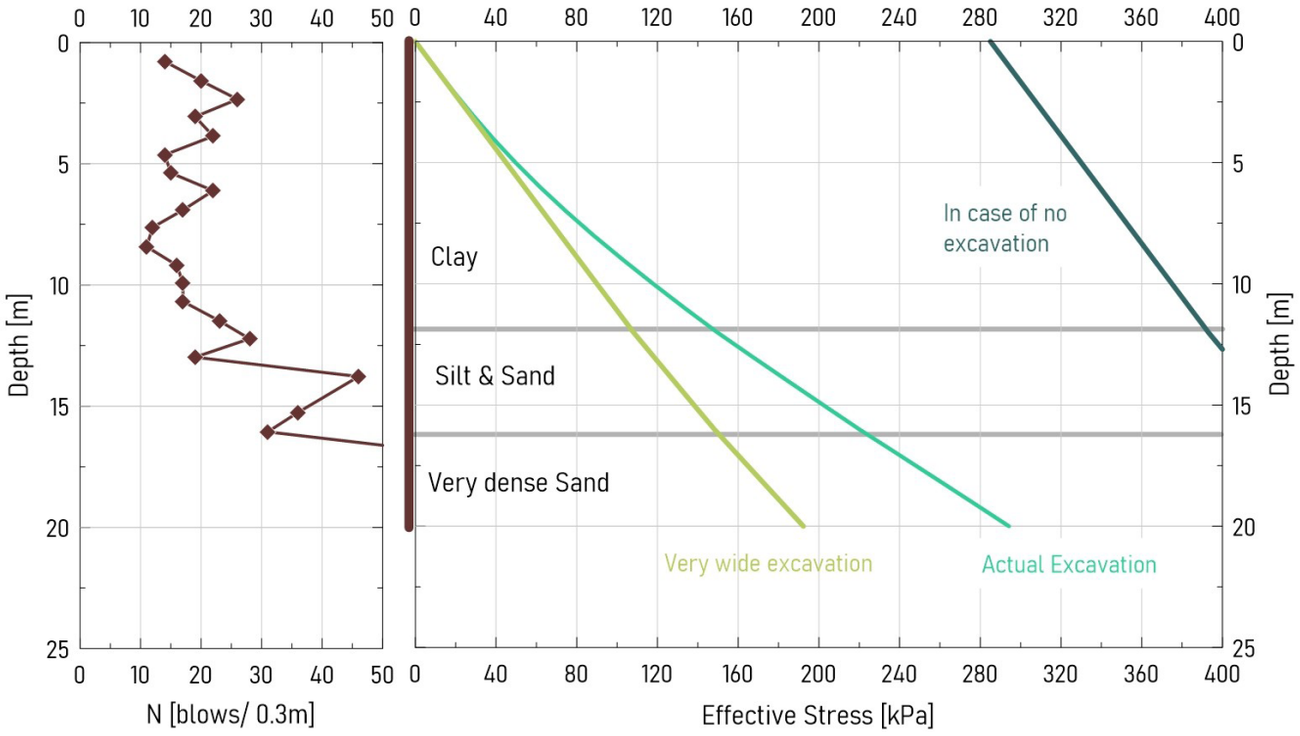

Figure 1. SPT -N profile and effective stress vs. depth at the test pile location

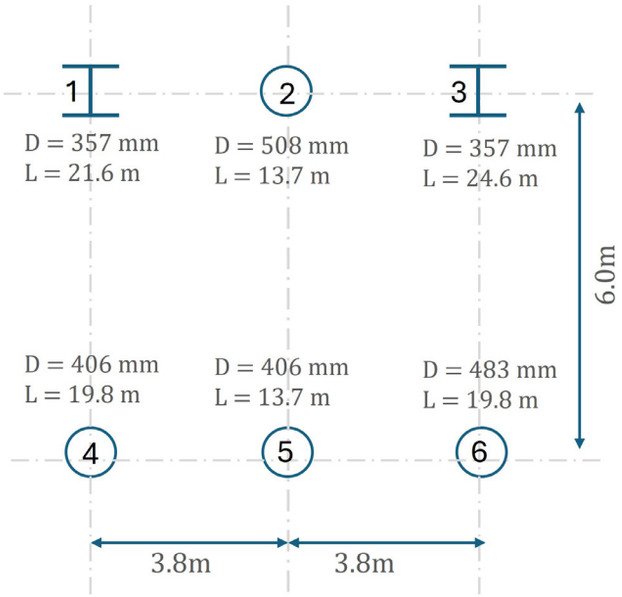

Figure 2. Site plan of test pile locations

dense sand, relative to the excavated surface. Groundwater conditions were maintained during testing using a system of well-points installed around the test site.

At the time, the standard approach was to conduct stress-independent (i.e., total stress) analyses. As a result, little consideration was given to the fact that, despite the relatively wide excavation, the effective stress distribution at the test site did not fully replicate that of the project site, as illustrated in Figure 1. (Note: zero depth is referenced at the bottom of the excavation. The unloading effect caused by excavation was estimated using Boussinesq stress distribution. Borehole logs and N-indices refer to measurements prior to excavation.)

The test program included six driven, telltale-instrumented piles: four closed-toe pipe piles and two 14-inch H-piles. The pipe piles had diameters of 16, 19, and 20 inches (406, 483, and 508 mm), as shown in Figure 2. The piles were installed near the center of the excavation, with the shortest distance to the excavation wall being 11 m. Embedment depths ranged from approximately 14 to 22 m. The wall thicknesses of the pipe piles were not reported in the original paper. Figure 2 illustrates the layout and dimensions of the test piles.

Three pipe piles (Piles 2, 4, and 6) were driven to depths of 19.8 m, while one (Pile 5) was terminated at 13.7 m in the silt and sand layer. The two H-piles (Piles 1 and 3) were driven to depths of 21.6 and 24.6 m, respectively. Pile 1 included a toe plate covering the full cross-section. The target sustained loads for the analysis were 900 kN in compression and 400 kN in tension.

All six piles were instrumented with telltale rods, evenly spaced along the pile length. The telltales were housed in two protective U-channels—three rods per channel—resulting in an approximate 11% increase in the pile's circumferential area. Measurements from the telltales were converted to strain and used to calculate axial force distributions along the pile during the static loading tests. The pipe piles were tested under both compression (push) and tension (pull) loading, while the H-piles were tested only in compression.

Test Schedule and Results

The loading tests commenced approximately two to three weeks after pile driving. The loading schedule generally consisted of applying load increments of 30 and 40 kips (133 and 178 kN), with each increment held constant for uneven durations. These were interspersed with intermediate unloading phases, also held for uneven lengths of time. Figure 3 illustrates the applied load versus time, along with the corresponding measured displacement over time for Pile 2 (data extracted from the scanned and digitized original report).

The somewhat irregular unloading–reloading sequence reflects the testing philosophy of the time, when it was believed that the pile head displacements recorded at multiple zero-load points could indicate toe movements under the maximum applied load. This assumption is now understood to be incorrect. Furthermore, modern practice recognizes that unloading–reloading cycles offer no meaningful insight and can significantly distort interpretation of data from instrumented piles—at times making it impossible to evaluate the instrumentation records reliably (Fellenius and Nguyen, 2019; Fellenius, 2024).

Figure 4 presents the original dual-graph format of the measured load–displacement results for Pile 6 (vertical axis in inches). It is notable that toe displacements exceeded 5 mm at applied loads beyond 3,200 kN (320 tons), suggesting that the shaft resistance was likely fully mobilized prior to reaching that load level.

Figure 5 presents the distribution of axial force in the same pile for various applied loads (in US customary units—feet and tons). Telltale rods are numbered 1 through 6. The force distributions were derived from the differentiation of the telltale measurements. The plots are supplemented with inset diagrams composed of sloping lines, where the decreasing slope with depth reflects increasing mobilization of unit shaft resistance.

Figure 6 provides a replot of Pile 6's load–displacement data from Figure 4, combining the original pair of graphs into a single plot to facilitate comparison between the compression (push) and tension (pull) tests. The vertical red bar in Figure 6 represents the range of evaluated "capacities" as determined by Mansur and Kaufman (1956), based on their three different definitions: (1) the load that produced a 6 mm (0.25 inch) net pile head movement after unloading, (2) the load defined by the intersection of initial and final linear approximations of the load–displacement curve, and (3) the load that caused a gross 6 mm (0.25 inch) pile toe displacement. The horizontal placement of the range bar was chosen so that the average of the three "capacity" values falls on the measured response curve. The original paper did not indicate a preferred definition, nor did it specify the factor of safety used or intended for the project.

The results from the original compression and tension tests presented in Figure 5 are synthesized in Figure 7. The x-marks labeled 1 through 6 within the "pile column" denote

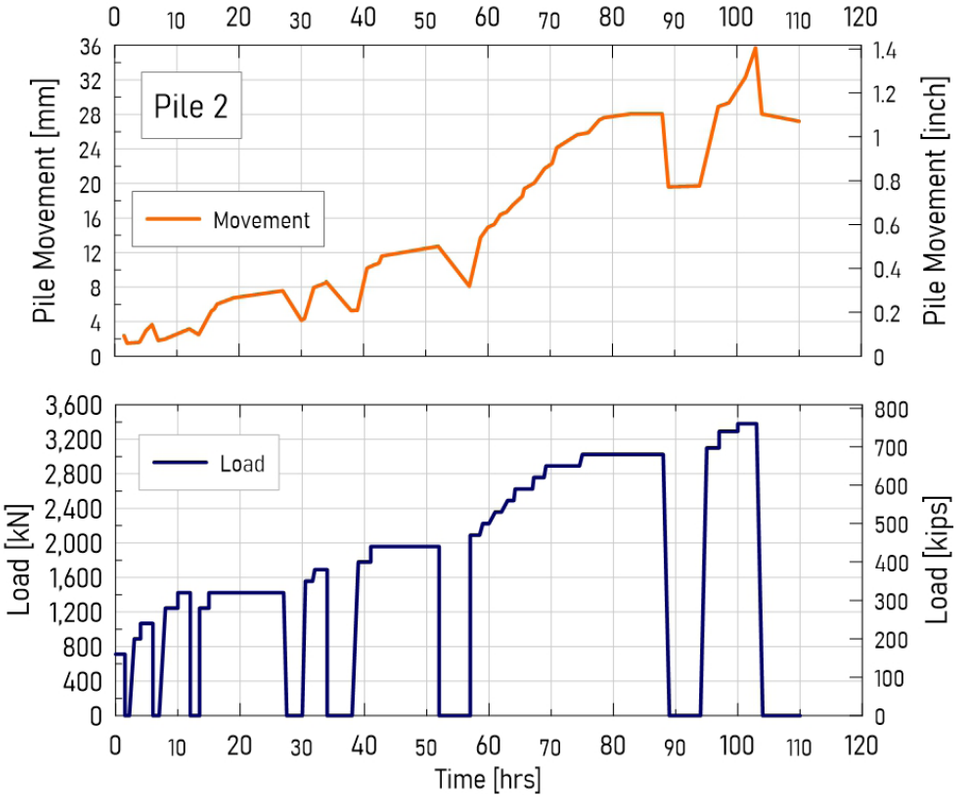

Figure 3. Load and measured movement vs. time for Pile 2, compression test

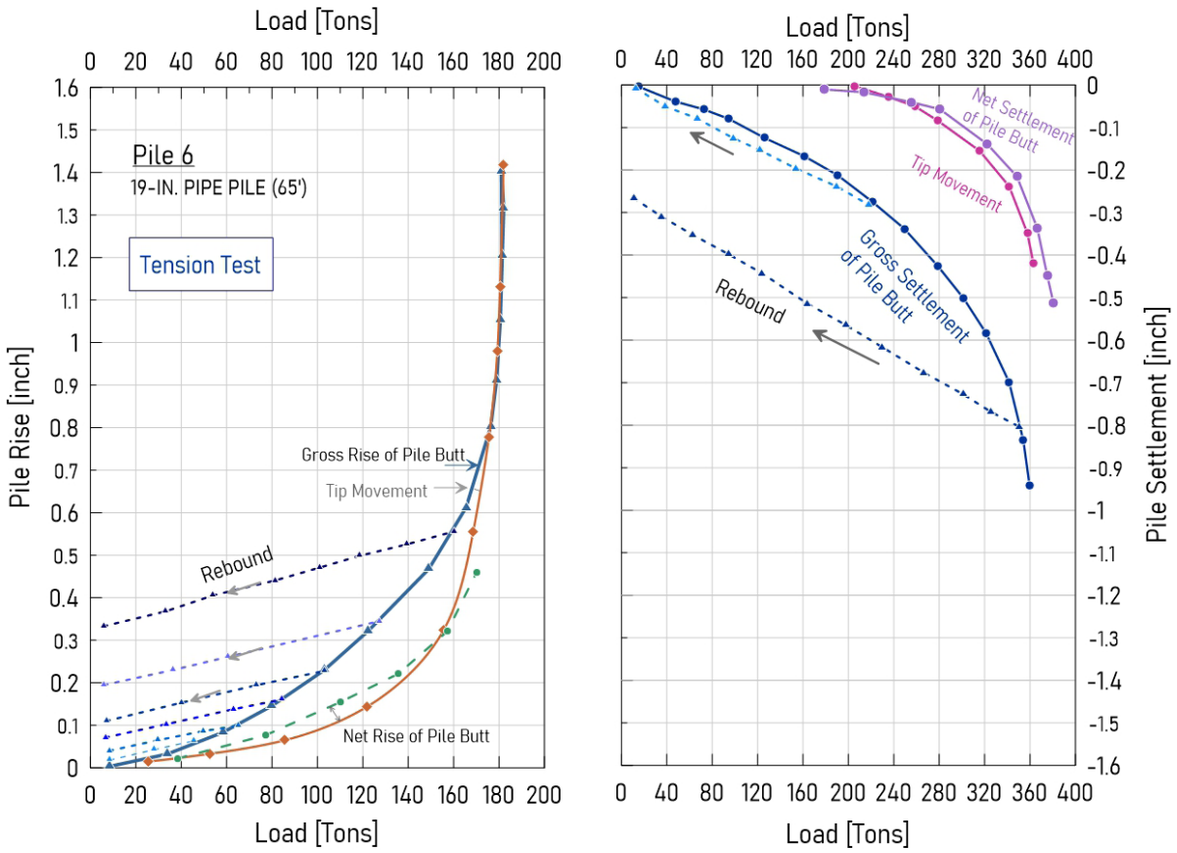

Figure 4. Load-movements measured for Pile 6 in pull (left graph) and push (right graph) (redrawn after Mansur and Kaufman 1956)

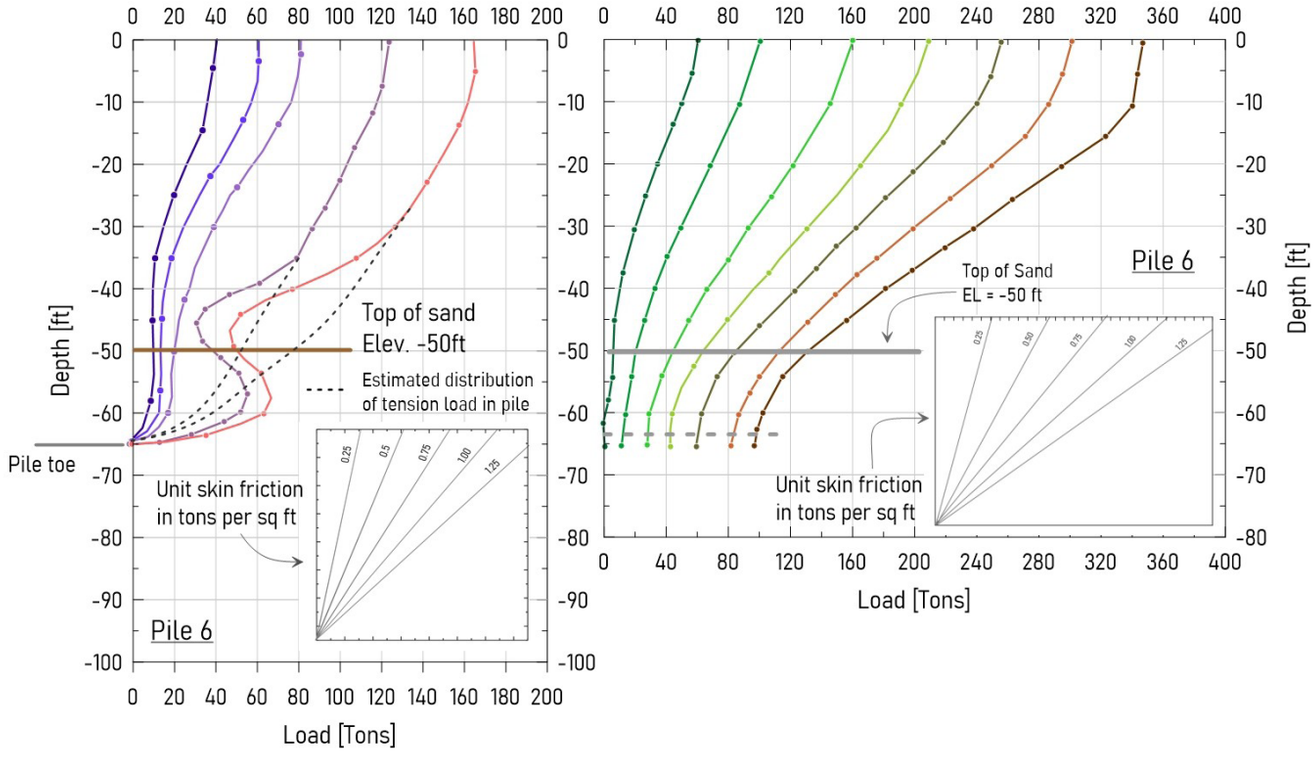

Figure 5. Force distribution reported for Pile 6 in pull (left graph) and push (right graph) (redrawn after Mansur and Kaufman 1956)

the locations of the telltale terminations. The force distributions depicted in Figures 4 and 6 were derived by differentiation; specifically, they were calculated based on the measured shortening between adjacent telltales, with the resulting force values plotted at the midpoint between the respective telltale ends. Except for the force profiles derived from the pull-test measurements between Telltales 3 and 4 (represented by dashed lines), the data exhibited minimal scatter. The records associated with Telltale 3 appear to be unreliable, indicating that the force values inferred from the difference between Telltales 2 and 3 cannot be considered accurate. Notably, the original publication did not substitute the suspect Telltale 3 data by using the differential measurement between Telltales 2 and 4.

The pull-test curves presented in Figure 7 suggest the presence of a tensile resistance at the pile toe during the pull test—an outcome that, from a mechanical standpoint, is not feasible. Mansur and Kaufman (1956) failed to recognize that the apparent development of significant force and shear resistance near the pile toe (as indicated by Telltales 1 and 2) during the pull test was the result of a locked-in, or residual, force remaining in the pile following the preceding compression (push) test. Contrary to this interpretation, they explicitly stated that no residual force was present in the pile at the onset of the push test. Due to their confidence in the telltale-based force calculations, Mansur and Kaufman further accepted the pronounced variation in shaft resistance magnitudes between the silt/sand layers and the dense sand layer. They interpreted these results as indicative of lower shaft resistance during pull relative to push, without accounting for the residual forces that had influenced the push test results as well. It is important to note that during the 1950s, the concept that pile installation often introduces residual forces into the foundation system had not yet been widely recognized.

The reported discrepancy between shaft resistance in tension and compression, as presented by Mansur and Kaufman (1956), has been referenced in subsequent literature as a true difference between push and pull conditions. Indeed, even to this day, some practitioners maintain that negative (uplift) shaft resistance in sand is inherently lower than positive (compression) resistance. However, this misinterpretation stems from a failure to consider the influence of residual force present within the pile prior to static testing. This oversight was subsequently identified by Hunter and Davisson (1969) and later substantiated through direct experimental evidence by Gregersen et al. (1973).

Figure 8 illustrates the axial force profiles along four instrumented pipe piles at the peak applied load of approximately 3,000 kN. The measured force distributions, indicated by blue markers and corresponding solid blue curves, demonstrate a high degree of consistency across all piles. These empirical results are compared with several modeled distributions derived from effective stress-based curve fitting.

The solid red curves represent analytical simulations calibrated to the measured push test data, with residual forces

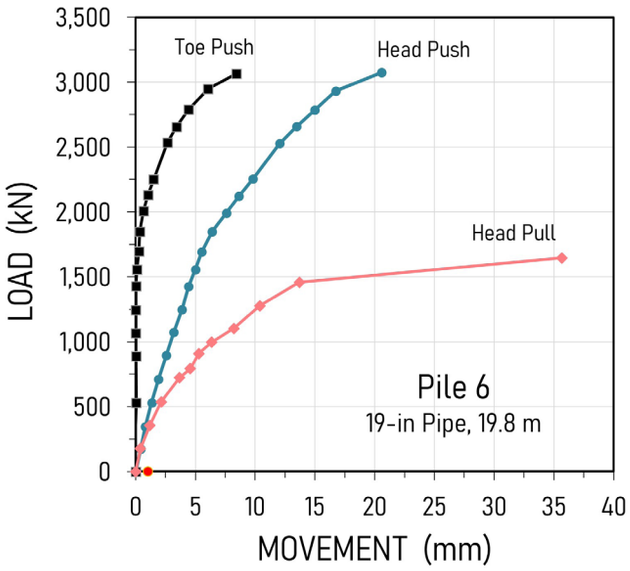

Figure 6. Load-movements measured for Pile 6 in push and pull direction, extracted and redrawn from Figure 4

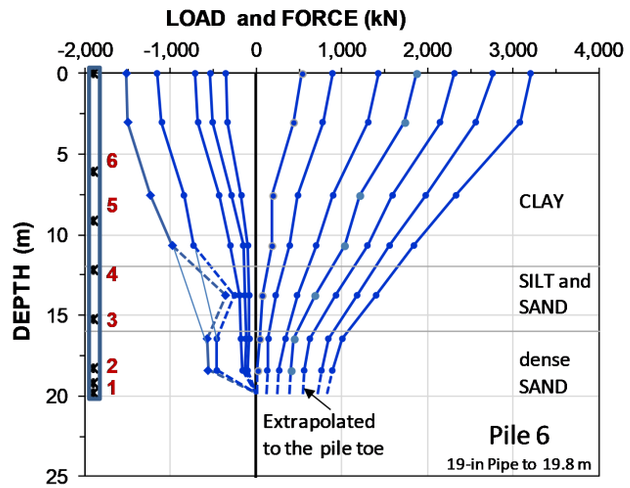

Figure 7. Replot of force distributions reported for Pile 6 in push and pull

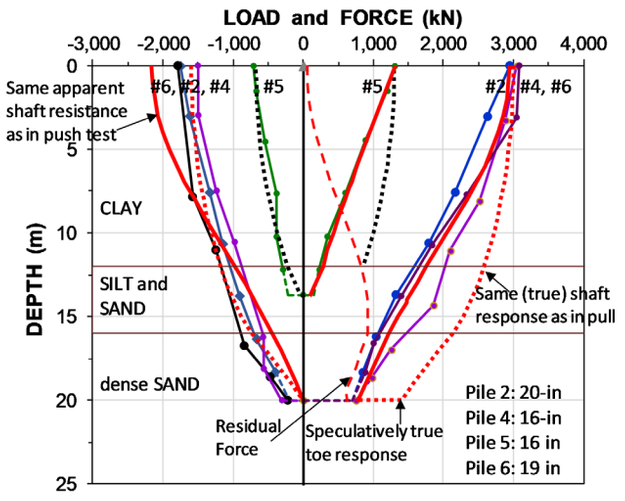

Figure 8. Calculated and simulated force distributions

left unadjusted. The same shaft resistance parameters from this calibration were applied to simulate the pull test behavior. A separate curve, shown with red dots, was fitted to the averaged pull test data and then projected onto the push test scenario. This representation serves to approximate the force distribution that would be expected if the shaft resistance observed in the pull test also governed the push test response, thereby including an estimate of the true toe resistance.

Further comparisons include a red dashed curve, which reflects the push test response of Pile 5 using a consistent set of β-coefficients, and a green dotted curve representing the corresponding fit to its pull test data. Together, these modeled distributions offer insight into the consistency of shaft behavior and highlight the significance of residual forces in interpreting loading test results.

The back-calculated β-coefficients corresponding to the maximum applied load during the push tests were approximately 1.2, 0.6, and 0.4 for the clay, the silt and sand, and the dense sand layers, respectively. For the pull tests, the average β-values were found to be 0.4, 0.5, and 0.8 in those same layers. The values derived from the pull test data are likely closer to the actual in-situ shaft resistance, as they appear to be less influenced by residual forces. Notably, these coefficients are somewhat higher than typically reported for comparable soil conditions under similar relative displacements. This deviation may be attributed to preloading effects, as the 15-meter site excavation prior to testing likely introduced a pre-stressed condition in the surrounding soil mass.

The magnitude of residual force inferred from the push test distributions—represented by the vertical separation between the solid and dotted simulation curves—exceeds the mobilized shaft resistance. This discrepancy highlights a degree of uncertainty in the test data, which is not unexpected given the limitations of telltale-based measurements and the inherent variability introduced by the differentiation process used to derive force distributions. It is plausible that the computed forces from telltale strains underestimated the actual internal forces to some extent.

In their original analysis, Mansur and Kaufman (1956) estimated ultimate unit shaft resistance within the silt and sand and the dense sand layers by correlating to average effective vertical stress (σ′) and assigning representative friction angles (ϕ′) of 28° for the silt and sand, and 36° for the dense sand. These parameters were incorporated into the conventional expression for shaft resistance, $r_s = \sigma' \cdot K \cdot \tan \phi'$ r_s, leading them to conclude, mistakenly, that the average earth stress coefficient (K) was 1.6 under compression and 0.6 under tension. However, this interpretation did not account for the presence of residual forces in the push tests, which likely caused a significant overestimation of shaft resistance in compression.

Figure 9 presents the load–displacement curves at the pile head for all tested pipe piles. The alignment of load–movement behavior across the three equal-length piles is notably consistent. The dashed red curve represents the simulated response of a 19-inch diameter pipe pile using the β-coefficients calibrated to the push test data. The red dotted curves correspond to simulations using the β-values derived from the pull test data. Additionally, the curve labeled "6 head-toe" illustrates the simulated end-bearing response of Pile 6, modeled with a pile wall thickness of 3/8 inch.

The simulations are made for a 12-mm relative pile-soil movement, a "target" value, using the same hyperbolic t-z function for all pile elements. At a 5-mm target movement, the beta-coefficients producing the same load-movement fit would be 75 % of those indicated.

Figure 10 presents the axial force–movement relationships. The blue curves represent digitized records extracted from the original publication, while the red curves correspond to numerical simulations calibrated to the push test data, incorporating the effects of residual force. Accurately fitting analytical curves to measurements influenced by residual force presents a notable challenge, as residual force is

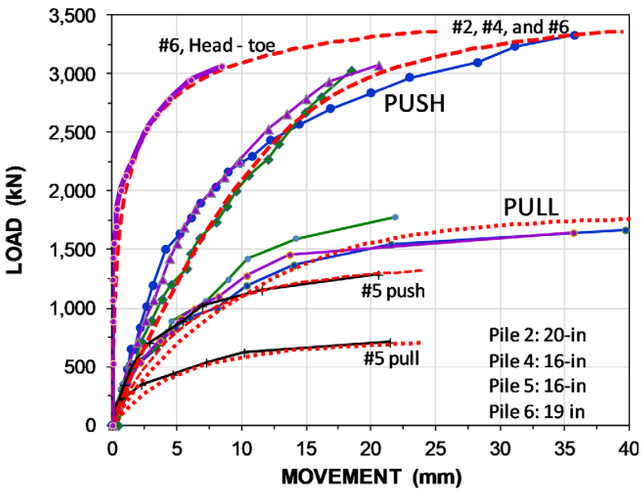

Figure 9. All push and pull load-movement curves plotted together

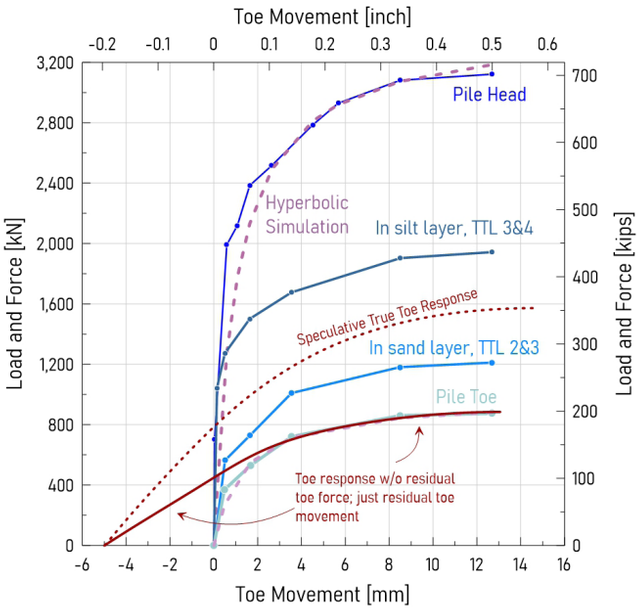

Figure 10. Force-movement records vs. measured pile toe movement

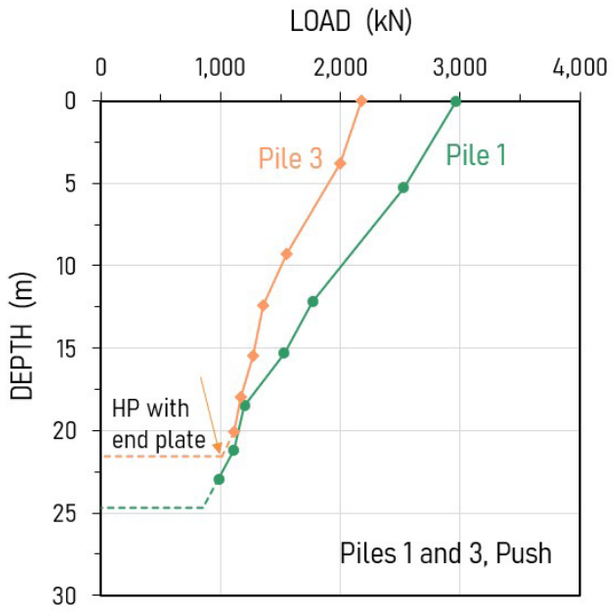

Figure 11. Force distribution back-calculated for the H-piles at the maximum applied load

inherently coupled with residual displacement. In contrast, simulation frameworks typically assume that the interface shear resistance between the pile and surrounding soil is zero at the commencement of loading—a condition that does not reflect the actual preloaded state of the system.

In the upper portions of the pile shafts, the observed response reflects an initial condition influenced by prior negative (uplift) movement, which gradually transitions to positive direction movement as the applied load increases during the test. In contrast, the lower segments of the piles exhibit initial conditions characterized by prior positive movement, and the shear resistance along these zones rapidly reaches or is already at full mobilization. A detailed discussion of these mechanisms is provided in Fellenius (2015; 2025).

The toe response under the influence of residual force is also distinct. When the loading test starts, the soil is in a prestressed state, causing the toe force to rise steeply with minimal displacement. Once the applied stress exceeds the pre-existing stress level, the response reverts to a path that aligns with the undisturbed (virgin) load–movement relationship. In Figure 10, the solid red curve traces the actual observed displacement trajectory, while the dot-dashed curve approximates the idealized virgin response that would occur in the absence of residual stress.

Piles 1 and 3, both H-section piles, were identical in geometry except for the presence of a toe plate on Pile 3. Figure 11 presents the back-calculated axial force distributions corresponding to the maximum applied load for each H-pile. The results exhibit general load transfer behavior consistent with that observed in the pipe piles, thereby supporting the applicability and reliability of the analytical approach.

The data suggest that the addition of the base plate did not enhance toe resistance, as no increase in toe-bearing force is evident in the distribution for Pile 3. Instead, the steeper gradient in the force profile along the shaft of Pile 3 implies a reduction in mobilized shaft resistance. This trend persists even when accounting for the influence of residual forces, reinforcing the interpretation that the toe plate altered the load transfer mechanism by decreasing shaft resistance rather than contributing to base resistance.

Conclusions

The seminal work by Mansur and Kaufman (1956) was among the first to demonstrate the value of instrumenting test piles to capture internal force distributions, thereby enabling the separation of shaft resistance from toe resistance. This approach provided a significantly more informed understanding of pile response than could be achieved by relying solely on pile-head load–displacement measurements. The authors examined the mobilized shaft resistance under both compressive (push) and tensile (pull) loading and reported a difference in response between the two modes. However, they did not recognize the influence of residual forces within the test piles, which led to the erroneous conclusion that shaft resistance mobilized in tension was inherently lower than that mobilized in compression. The role of residual forces in these tests was later identified and addressed by M.T. Davisson in a re-analysis of the same dataset (Hunter and Davisson, 1969). Furthermore, the original study did not consider the impact of the 15 ft (approximately 5 m) excavation of overburden prior to testing, which likely contributed to elevated unit shaft resistance through preloading effects.

This publication was also one of the earliest to advocate for interpreting static loading test results in terms of the force–movement behavior of pile segments and the resulting foundation settlements, rather than relying solely on predefined notions of capacity accompanied by global safety or resistance factors. The approach laid important groundwork for the evolution of performance-based piled foundation design.

Although the proposed lock and dam structures for which the tests were conducted were ultimately to be supported by large pile groups, the paper did not address the differences in response between isolated single piles, as tested, and group pile behavior. The authors noted that the compressive and tensile capacities of piles installed in groups may exceed those observed in single-pile tests due to increased subgrade densification during group installation. While this may be valid for "capacity", group settlement response is governed by stress distribution and the compressibility of the soil strata below the pile toe, rather than by soil–pile interaction along the embedded shaft above the toe level.

References

Feagin, L.B., 1948. Performance of Pile Foundations of Navigation Locks and Dams on the Upper Mississippi River. Proceedings, Second International Conference on Soil Mechanics and Foundation Engineering, Rotterdam, Vol. IV, pp 98-106.

Fellenius, B.H., 2015. Static tests on instrumented piles affected by residual force. Journal of the Deep Foundation Institute 9(1) 11-20.

Fellenius, B.H., 2025. Basics of foundation design—a textbook. Electronic Edition, www.Fellenius.net, 572 p.

Fellenius, B.H. and Nguyen, B.N., 2019. Common mistakes in static loading-test procedures and result analyses. Geotechnical Engineering Journal of the SEAGS & AGSSEA, September 2019, 50(3) 20-31.

Gregersen, O.S., Aas, G., and DiBiagio, E., 1973. Load tests on friction piles in loose sand. Proc. of 8th ICSMFE, Moscow, August 12-19, Vol. 2.1, Paper 3/17, pp. 109–117.

Hunter, A.H. and Davisson, M.T., 1969. Measurements of pile load transfer. Proc. of Symposium on Performance of Deep Foundations, San Francisco, June 23-28, 1968, American Society for Testing and Materials, ASTM, Special Technical Publication, STP 444, pp. 106-117.

Mansur C.L. and Kaufman, R.I., 1956. Pile tests, low sill structure, Old River, Louisiana. Pile tests, low sill structure, Old River, Louisiana, Transactions, ASCE J. 82(10) 715-744.

Mansur, C.L., Hunter, A.H., and Davison, M.T., 1964. Pile driving and loading tests. Lock and Dam No. Report by Fruco and Associates to US Army Corps of Engineers. 209 p.

Mansur C.I. and Hunter, A.H., 1970. Pile tests–Arkansas River project. ASCE J. 96(SM5) 1545-1582.